Hindawi
Advances in Civil Engineering
Volume 2022, Article ID 5219261, 12 pages
https://doi.org/10.1155/2022/5219261

Research Article

Shaking Table Tests on Wrap Rope Connect Device for Continuous-Beam Bridges with Different Pier Heights

Yanfang Liu,[1,2] **Wenxue Zhang**,[1] **Xiuli Du**,[1] **and Weigang Bao**[2]

[1]*College of Architecture and Civil Engineering, Beijing University of Technology, Beijing 100124, China*
[2]*China Communications Construction Company Limited, Beijing 100088, China*

Correspondence should be addressed to Yanfang Liu; 21s033014@stu.hit.edu.cn

Received 13 March 2022; Accepted 20 July 2022; Published 25 August 2022

Academic Editor: Carlo Rainieri

To investigate the cooperative and isolation effectiveness of the wrapped rope connect device (WRCD) on continuous-beam bridges with different pier heights, shaking table tests were conducted on a typical three-span continuous-beam bridge model. The model had additional pier stiffness and applied the WRCD. Two actual seismic waves with different spectral characteristics and multiple intensities were used for input ground motion. By examining the performance and measured structural response under various excitations, WRCD could effectively improve the overall cooperative effect of the model structure for a limited increase in the input seismic energy of the system. The acceleration ratio from the fixed pier top to the movable pier top increased from~17% without the WRCD to~32% with it. The strain-response ratio of the pier bottom decreased from its maximum of 24.8 times to 3.6 times after the device was applied. There is a specific relationship between the influence and the pier height of the structure, and the rules for high and low piers slightly differ. The movable and fixed ports can be coordinated by setting reasonable design parameters of the WRCD, which can be used for the seismic design of continuous-beam bridges with different pier heights.

1. Introduction

With the rapid development of traffic construction in western China, many continuous-beam bridges with different pier heights have been developed to adapt to the steep terrain in mountainous areas. Earthquakes frequently occur because of plate-related movement in west China; therefore, earthquakes have become the primary factor controlling bridge structure design. Because of the different pier heights, the longitudinal stiffness of the pier structure is not coordinated. Furthermore, the conventional continuous-beam bridge usually only sets one joint as the fixed support; therefore, the seismic inertial force of the superstructure, distributed according to the pier stiffness, is primarily focused on the pier at this fixed asset. The use of single fixed support severely tests the seismic design of continuous-beam bridges. Although a plastic hinge can be set at the pier with limited license by increasing the ratio of reinforcement and the flexibility of the dock can be used to improve the structure's seismic performance, this method inevitably produces damage that is difficult to repair. The most common seismic design method of continuous-girder bridges is to set multiple seismic isolation bearings. Many studies have been conducted on damping measures, such as damping isolation bearings and viscous dampers for continuous-girder bridges, and many research results have been achieved [1–3]. However, regardless of the type of isolation bearings adopted, a large relative displacement must be applied to accomplish the ideal damping effect [4, 5]. In recent years, sure researchers have conducted systematic studies on lock-up devices; then, lock-up connections cannot effectively reduce the impact of seismic activity on low-pier continuous-girder bridges [6–10]. Moreover, owing to cost and late maintenance, there are not many applications in practical engineering.

In order to improve the longitudinal cooperative forces of high continuous-girder bridges with unequal piers and enhance the longitudinal seismic performance of continuous-girder bridges, a winding cable mechanism was proposed for the purpose of cooperative forces [11, 12]. The

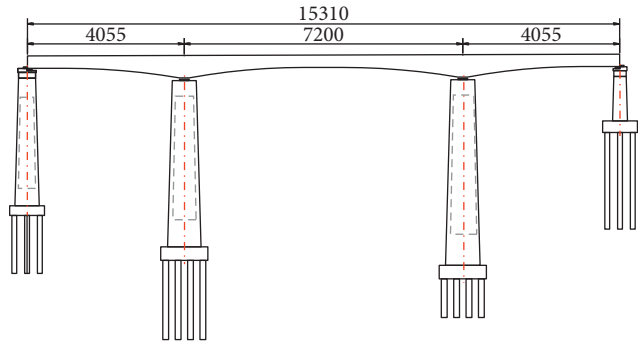

Figure 1: Bridge span arrangement of the prototype (unit: cm).

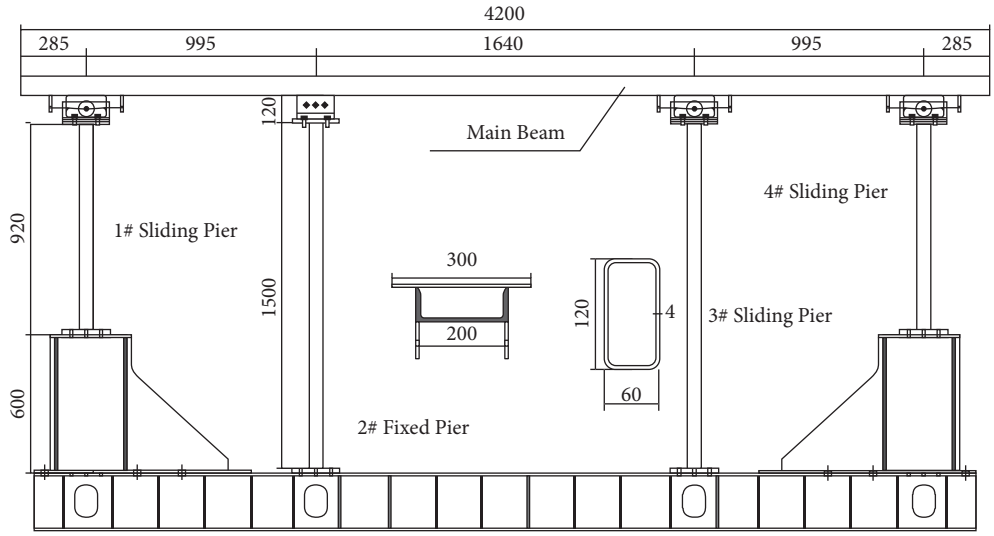

Figure 2: Arrangement of the bridge model.

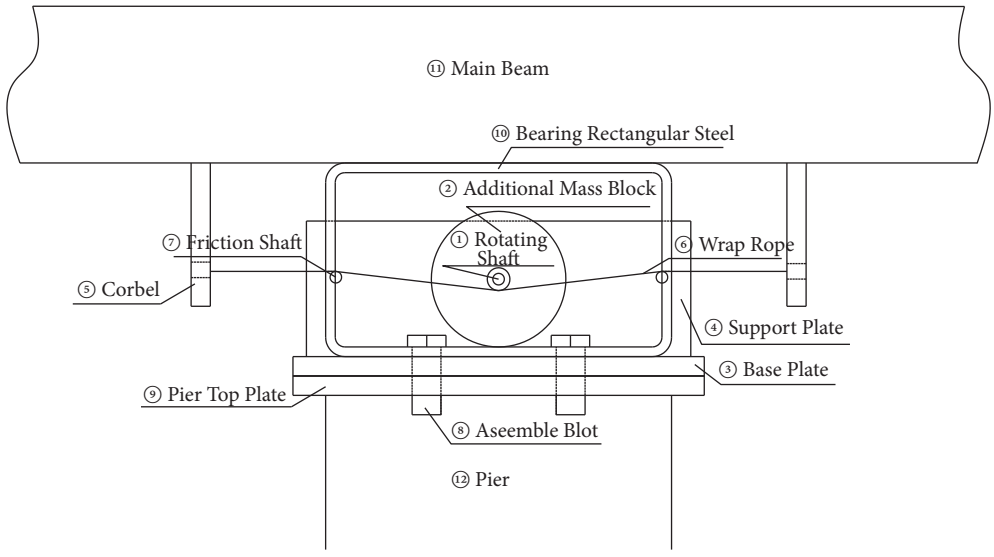

Figure 3: WRCD structural diagram.

device can achieve the synergistic force effect and meet the purpose of energy dissipation and displacement control. Meanwhile, it is a new type of cable winding device with the instantaneous locking performance of lock-up devices and energy dissipation performance of damping measures. The shaking table test of a typical straight-girder bridge was performed. By analyzing the seismic response of the bridge structure under different spectral characteristics and ground

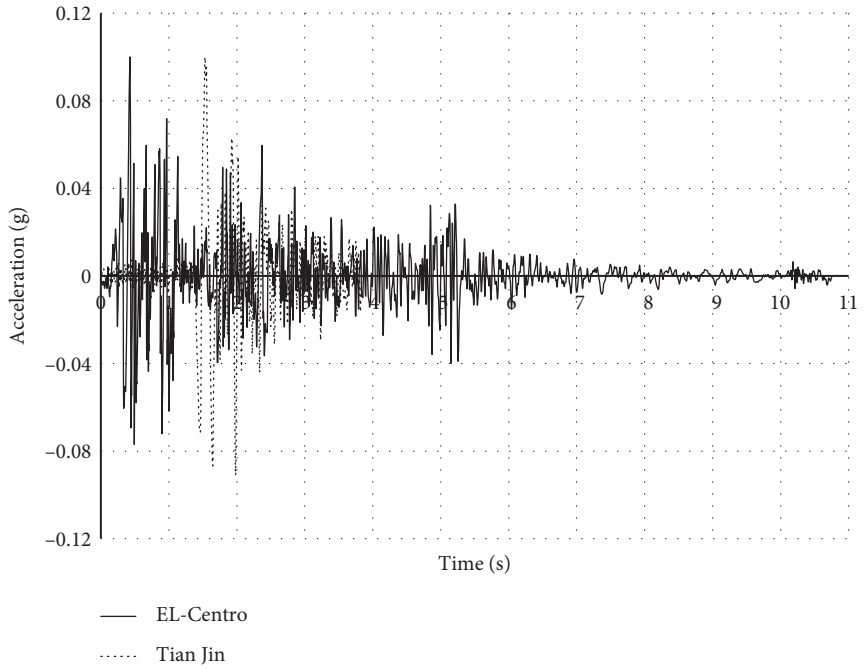

Figure 4: Acceleration time history of input earthquakes.

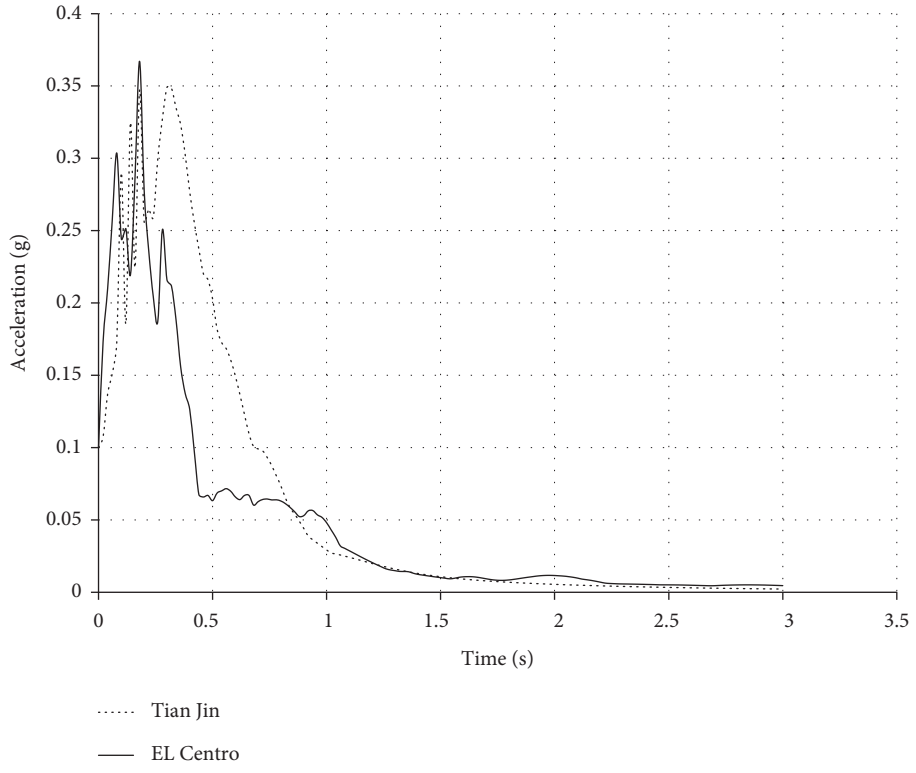

Figure 5: Acceleration response spectra of input earthquakes.

motion excitations of varying input intensity, the joint force and damping effect of the WRCD were examined, and the applicability of the device in high continuous-beam bridges with unequal piers was confirmed to provide a reference for its application in similar bridge structures.

2. Shaking Table Test

2.1. Model Design. A typical three-span continuous-beam bridge with different pier heights, span 40.55 + 72 + 40.55 m, was considered as the research subject, as shown in Figure 1.

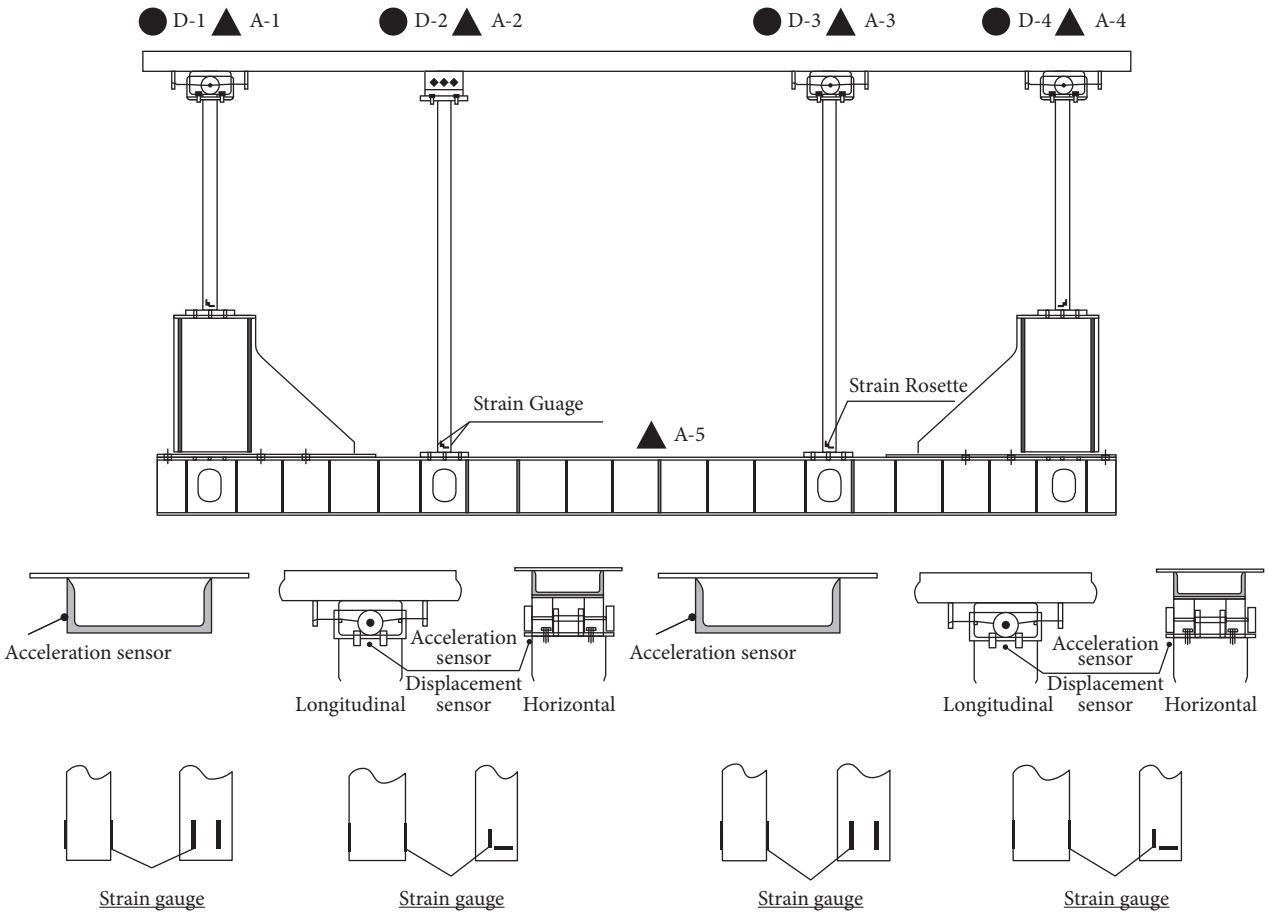

Figure 6: The layout of sensors in the bridge model.

Table 1: Natural frequency of two test model.

Working condition	Without WRCD (Hz)	With WRCD for 1C (Hz)	With WRCD for 2C (Hz)	With WRCD for 3C (Hz)
Before loading	3.649	4.305	4.303	4.304
0.6 g	3.644	3.650	3.645	3.647
0.8 g	3.636	3.649	3.656	3.643
1.0 g	3.628	3.653	3.650	3.649

The length similarity constant of the design model is 1/30, the acceleration similarity constant is 1, and the elastic modulus similarity constant is 6.338. Figure 2 shows the overall layout of the model bridge. The whole bridge model comprises a steel structure to avoid the uncertainty of concrete material parameters. The primary beam of the test model has a box section welded from section steel and steel plate. The bridge pier of the model assumes stiffness equivalence [1, 13–17]. The section design of the bridge pier is strictly equivalent as per the bending stiffness, ignoring the torsional and axial stiffnesses. The section is equal to the rectangular tube section. To ensure that the dynamic characteristics of the test model are similar to those of the original bridge, artificial mass is added to ensure that the structure meets the condition of mass similarity. The weight of the main beam of the model is 840 kg, and the importance of the pier varies as per the height of the dock. The consequences of the high and low ports are 100 and 40 kg, respectively.

2.2. WRCD Design. The WRCD comprises a rotating shaft ①, additional mass block ②, device backing plate ③, support plate ④, leg ⑤, winding cable ⑥, friction shaft ⑦, and assembly bolt ⑧. The device is proposed based on the principle, which uses the friction between the rope and the wooden pile to form a self-locking system. When there is a relative movement trend, it can produce greater friction. Euler proposed a formula between the friction and the number of turns of the rope around the wooden pile:

$$f_\mu = F_1\left(e^{2\pi\mu m} - 1\right)F_2 = F_1 e^{2\pi\mu m}, \quad (1)$$

where: f_μ is the friction force of winding cable; F_1 is the active tension the winding cable; F_2 is the passive tension of the winding cable; μ is the sliding friction coefficient between the winding cable and the cylinder; m is the number of winding turns.

The device considers the relative acceleration of the pier and beam as the control variable under the action of the

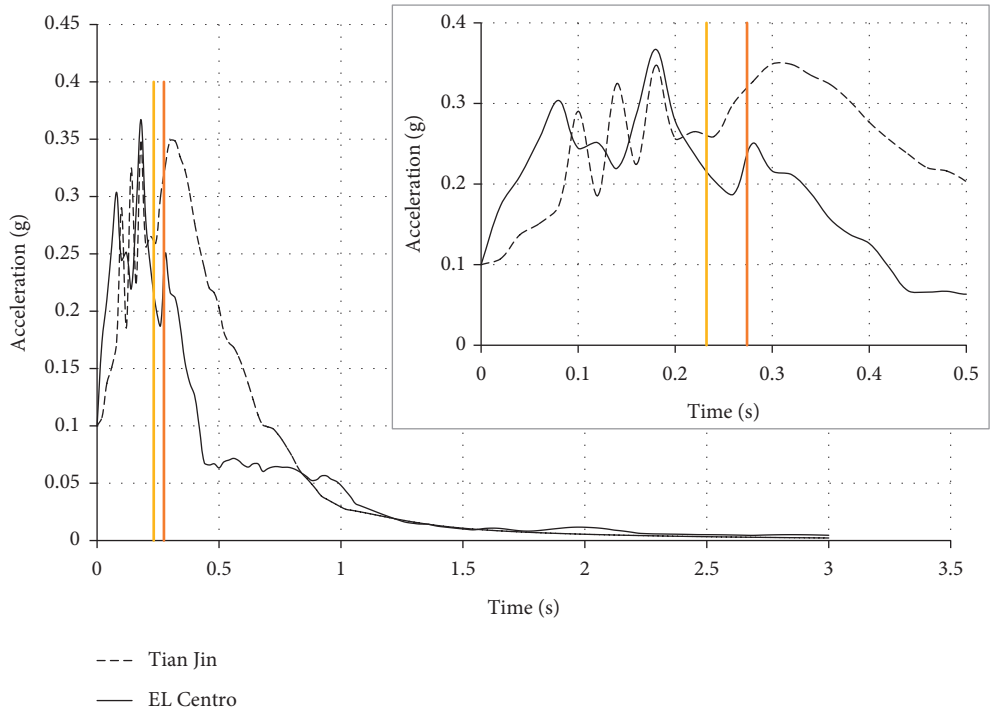

Figure 7: The relative relationship between the base vibration frequency and input response spectrum.

earthquake, uses the rotational inertial force of the additional mass of the rotating shaft to activate the coiled cable, and generates greater friction by rubbing the coiled rope on the post such that the pier of the movable support can reach the instantaneous "fixed" state, as shown in Figure 3. Furthermore, the seismic response of the superstructure is borne by portable and fixed-bearing ports, which reduce the seismic response of the fixed-bearing piers and the longitudinal displacement of the beam ends to improve the seismic performance of continuous-girder bridges [14]. When the earthquake input energy is considerable, friction in the coiled cable can consume a part of the input energy, which provides shock absorption.

2.3. Ground Motion Input. EL Centro (class ii) and Tianjin (class iv) waves were selected as the experimental seismic inputs. The length of both seismic waves has been compressed to a third of their original size. Figures 4 and 5 show the acceleration time-history and response-spectrum curves, respectively, of these two seismic waves after processing the peak acceleration and adjusting the input time.

2.4. Sensor Placement. A total of 37 sensors are arranged to test the model's dynamic characteristics and seismic response. The sensor layout is shown in Figure 6. Five accelerometers are used to measure the acceleration of the beam end, pier top, and mesa. Four cable displacement gauges measure the absolute displacement of the primary beam and the top of the pier. Four strain flowers (3 channels for each strain flower), and sixteen strain gauges were symmetrically arranged at the bottom of the dock.

3. Test Results and Analysis

3.1. Dynamic Property. To examine the influence of the number of windings on the friction axis of the WRCD on the damping effect of the structure, four models were designed: one with no WRCD and three with WRCDs with one, two, and three windings. Before each test, the form was swept with white noise to measure the natural vibration rate of the model and determine whether the dynamic characteristics of the system had changed. As per the strain measured at the bottom of the pier, the model steel member remains in the elastic stage during the test [18, 19]. Table 1 shows the dynamic characteristics of the four models under different peak acceleration conditions. The first-order natural vibration frequency is 3.649 Hz without a WRCD, whereas the natural vibration frequency was 4.305 Hz when the cable was wound for one turn, an increase of 18%. With increasing earthquake input intensity, the WRCD rotates, and the natural vibration frequency decreases from 4.305 Hz at the beginning to 3.65 Hz at 0.6 g, a decrease of ~15%. After rotation, the contribution of the device to the overall stiffness of the structure decreases, and the natural vibration frequency of the structure changes little with the earthquake input intensity. To summarize, under the condition of solid earthquake input, the design parameter of the WRCD after the rotation has no apparent influence on the natural vibration frequency of the structure, with a change rate of <1%. The experimental results of the dynamic characteristics of the model structure demonstrate that the overall stiffness of the model structure increases when the WRCD is adopted, and the overall cooperative force of the model structure is improved by the joint action of movable and fixed piers.

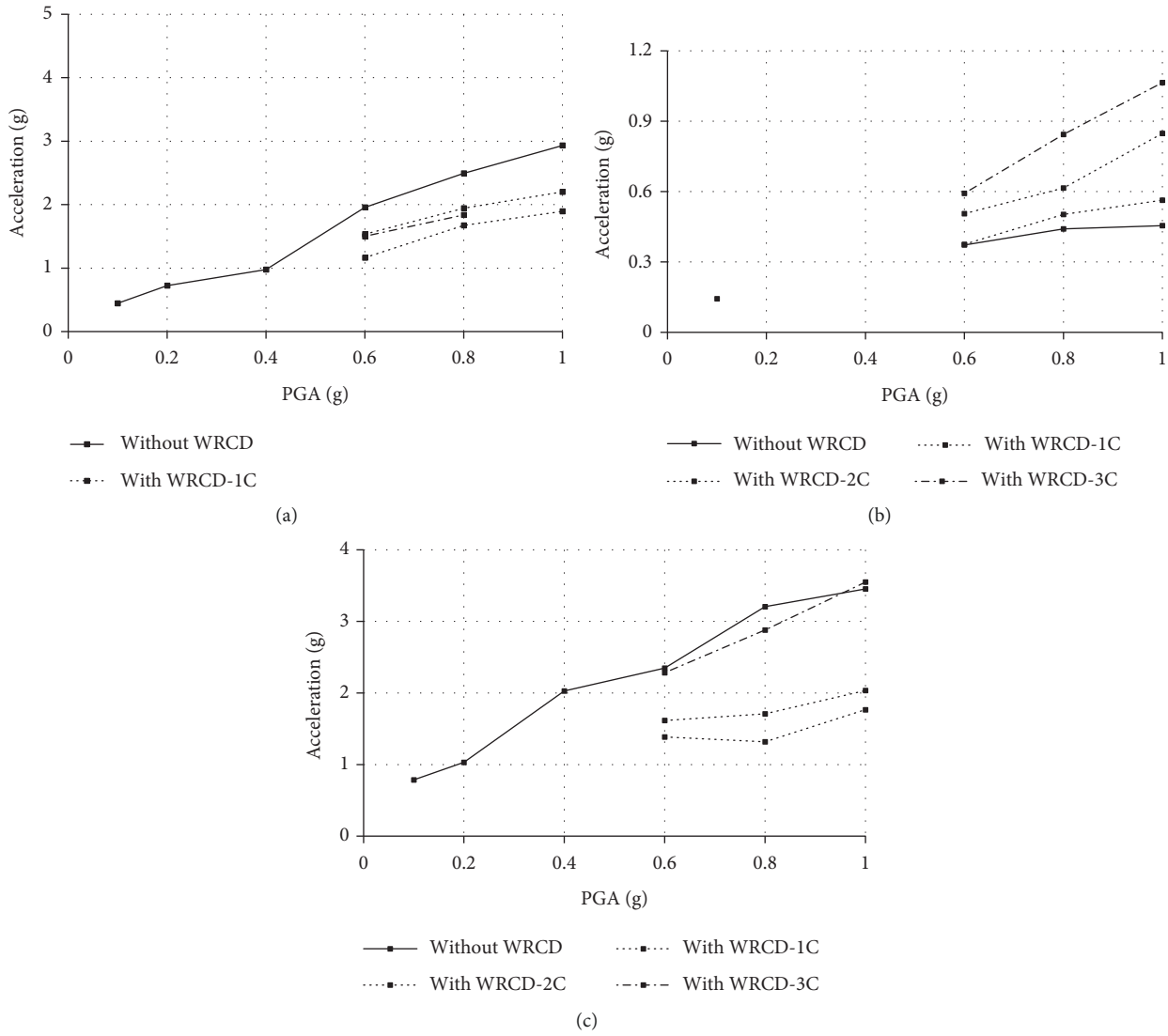

Figure 8: Acceleration variation trend with seismic input intensity under Tianjin ground motion. (a) Top of movable pier #1. (b) The main beam of pier #2. (c) Top of movable pier #3.

Figure 7 shows the relationship between the first-order vibration frequency of the model structure and the input ground motion response spectrum with and without the WRCD. The overall stiffness can be improved by the WRCD when the first-order dominant frequency of the model structure is in the platform segment of the input ground motion response spectrum. By increasing the input seismic energy of the system, the overall cooperative mechanical performance of the movable pier and the fixed pier of a continuous-girder bridge can be improved.

3.2. Acceleration Response. Figure 8 shows the variation trend of the maximum acceleration response at the top of the pier with seismic input intensity under the effect of the Tianjin wave. The acceleration responses of the active and fixed ports decreased and increased, respectively, without the WRCD. The impact of the number of windings on the acceleration response of the pier is inconsistent. The analysis demonstrates that for one winding, movable pier #1 ranged from −33% to −40.5%, whereas pier #3 ranged from −41% to −58.9%. With two windings, the acceleration responses of piers #1 and #3 are similar to those with one winding, and the acceleration responses of both pier tops decrease. Still, the extent of the decrease is not apparent. The acceleration response of pier #1 is from −21.6% to −24.9%, and that of pier #3 is from −31.2% to −46.7%. When the number of windings is one or two, the acceleration response of pier #1 decreased between −23.3% and −26.3%. However, the acceleration response of pier #3 fell less obviously than that of pier #3 when the number of windings was one or two with an amplitude between −2.7% and −10.2%.

In conclusion, the acceleration response of the WRCD to the active pier has a special relationship with pier height, and the influence of different numbers of windings on the high

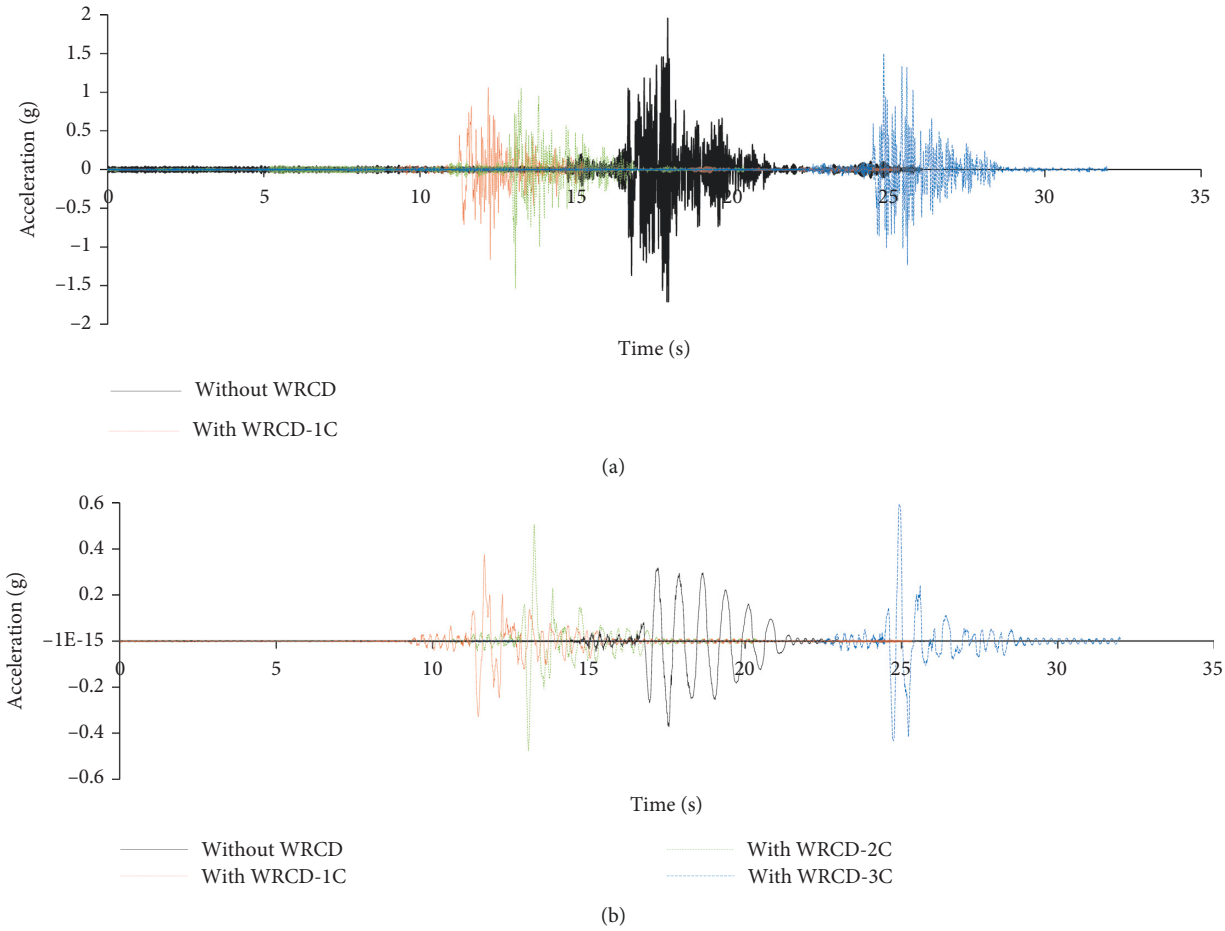

Figure 9: Acceleration time-history curve under Tianjin ground motion. (a) Time-history curve of the acceleration response of the top of active pier #1. (b) Time-history curve of the acceleration response of fixed pier #2.

and low docks differs. For fixed pier #2, the acceleration response of the pier top increases with increasing winding number, which is considerably higher than that without the device. Furthermore, the influence trend linearly rises with acceleration input intensity.

Figure 9 shows the time-history curves of the top acceleration of movable pier #1 and fixed pier #2. WRCD can improve the response characteristics of the model structure, and the responses of the portable and fixed piers are somewhat similar.

With a ground motion input of 0.8 g, the ratio of the acceleration response of the tops of fixed pier #2, movable pier #1, and portable pier #3 with and without the WRCD applied to the model structure are shown in Figure 10. Without the WRCD, the acceleration response of the top of the fixed pier is 17.7% and 13.7% of that of movable piers #1 and #3, respectively. When a WRCD with one winding is used, the response ratio increases to 30% and 38.1%. Therefore, the WRCD improves the collective mechanical performance of the movable and fixed piers. The balance of the acceleration response of fixed pier #2 to portable pier #1 increases with increased WRCD windings, indicating that the synergistic force effect of movable pier #1 and the fixed pier rises further. Finally, the response ratios of fixed pier #2

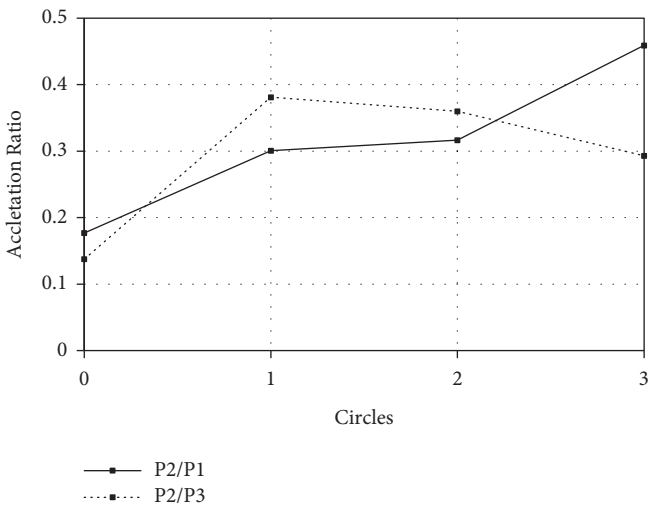

Figure 10: Acceleration ration relationship between piers under Tianjin ground motion.

and portable pier #3 first increase and then decrease with the increase in the number of windings; however, the proportions remain higher than those without the device. The

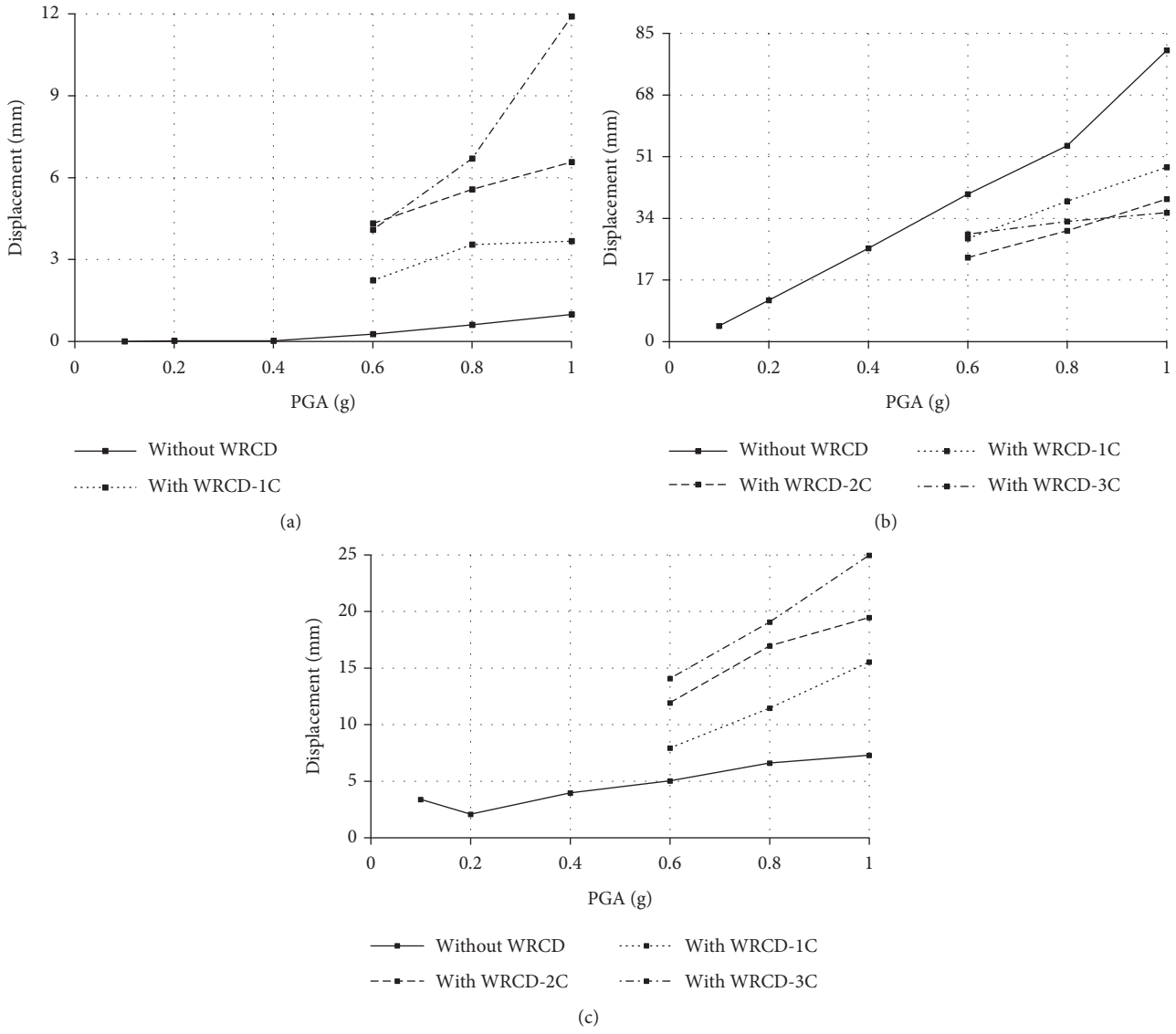

Figure 11: Displacement variation trend with seismic input intensity under Tianjin ground motion. (a) Top of movable pier #1. (b) the Main beam of pier #2. (c) Top of movable pier #3.

results demonstrate that the WRCD's effect on improving the movable pier's joint force is related to the stiffness of the portable port.

3.3. Displacement Response. Figure 11 shows the variation trend of maximum displacement at the pier top of each movable pier and the primary beam of the fixed port in response to the input intensity of in situ vibration under the action of the Tianjin wave. For #1 movable pier, the maximum response value of pier top displacement with WRCD is higher than that without WRCD. When the number of winding turns is one, the displacement response of the pier top increases from 7.3 times at 0.6 g to 4.8 times at 0.8 g, and finally to 2.7 times at 1.0 g. The synergistic stress effect of the movable piers becomes increasingly evident with the increase in earthquake intensity and increases with an increase in windings. The displacement increase with three windings is higher than those with one and two windings. The variation law of the pier top displacement response of movable pier #3 is similar to that of fixed pier #1; however, the relative variation range of displacement differs. For fixed pier #2 with WRCD, the displacement response of the main beam at the fixed pier is reduced compared with that without WRCD, and the maximum reduction ratio is 55%. The displacement reduction of two windings is better than that of one or three windings. The displacement response of the model structure demonstrates that when the WRCD is activated, the movable pier participates in the longitudinal force of the system and shares part of the inertial force of the primary beam, and the overall cooperative mechanical performance of the structure is improved.

3.4. Strain Response. Figure 12 shows the trend of the maximum strain response of the pier bottom under the effect of the Tianjin wave. The total strain response at the bottom

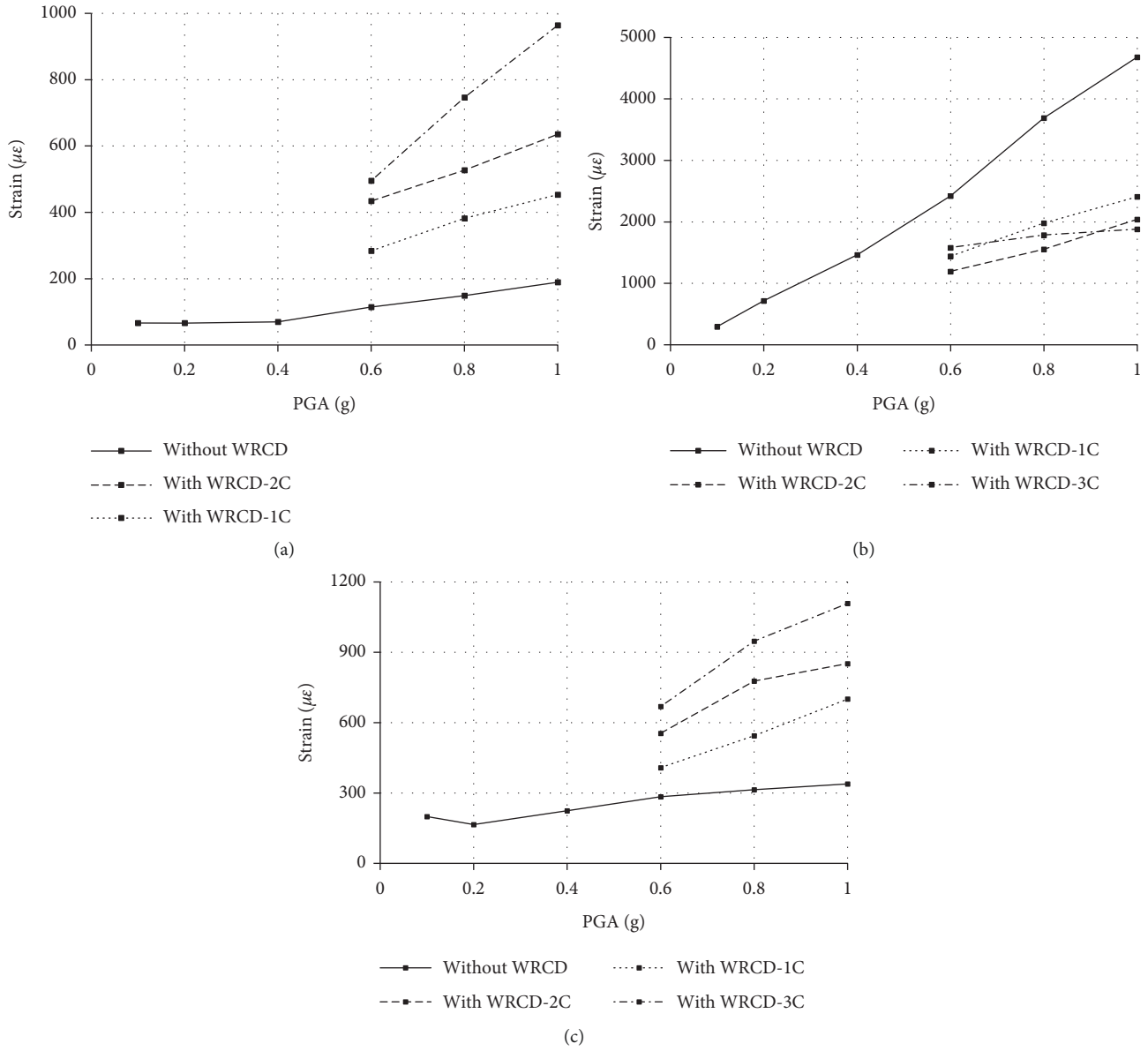

Figure 12: Strain variation trend with seismic input intensity under Tianjin ground motion. (a) Bottom of movable pier #1. (b) Fixed bottom of pier #2. (c) Bottom of movable pier #3.

of the movable pier increases after the WRCD is adopted. When the number of windings is 1, with the rise of ground motion input intensity, the maximum strain responses of movable piers #1 and #3 are 2.4–2.6 and 1.4–2.0 times those without the device, respectively. The results demonstrate that the response of the WRCD to the strain at the bottom of the active pier is related to the pier's height, and the strain response of the movable port at different sizes increases with increasing windings. The strain response of fixed pier #2 with WRCD is ~40% without WRCD. Under the same number of windings, the decrease in the strain response increases with the increase in seismic input intensity. The strain response of the pier bottom of the model structure shows that when the WRCD is activated, the active pier participates in the longitudinal force of the structure and shares part of the inertia force of the main beam and the overall cooperative mechanical performance of the structure is improved.

Under a ground motion input of 0.8 g, Figure 13 shows the proportional relationship of the pier bottom strain response of fixed pier #2 and movable piers #1 and #3 with and without WRCD in the model structure. Without the WRCD, the bottom strain response of the fixed pier is 24.8 times and 11.8 times those of movable docks #1 and #3, respectively. When the number of winding turns is one, the bottom strain response of the fixed pier is 5.1 times and 3.6 times that of the movable piers #1 and #3 when the number of winding turns is one. The corresponding ratio decreases with the increase in the number of windings. The experimental results show that the WRCD helps improve the collective mechanical performance of the

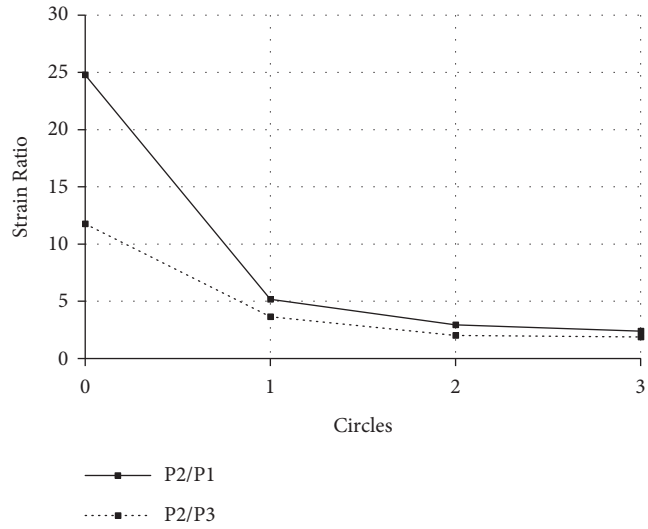

Figure 13: Strain ration relationship between piers under Tianjin ground motion.

Table 2: Maximum acceleration for different frequency spectra (g).

Peak acceleration (g)	Location	El centro (II)				Tianjin (IV)			
		Without WRCD	With WRCD-1C	With WRCD-2C	With WRCD-3C	Without WRCD	With WRCD-1C	With WRCD-2C	With WRCD-3C
0.8	P1	2.791	1.551	1.997	2.346	2.493	1.671	1.943	1.837
	P2	0.292	0.331	0.446	0.378	0.441	0.502	0.615	0.844
	P3	2.566	1.600	1.743	2.930	3.207	1.318	1.709	2.879

Table 3: Maximum displacement for different frequency spectra (cm).

Peak acceleration (g)	Location	El centro (II)				Tianjin (IV)			
		Without WRCD	With WRCD-1C	With WRCD-2C	With WRCD-3C	Without WRCD	With WRCD-1C	With WRCD-2C	With WRCD-3C
0.8	P1	0.212	2.258	3.570	2.589	0.610	3.552	5.570	6.696
	P2	31.640	14.406	12.306	13.019	54.002	38.696	30.552	33.154
	P3	4.046	5.649	5.777	7.202	6.603	11.464	16.963	19.076

Table 4: Maximum strain for different frequency spectra ($\mu\varepsilon$).

Peak acceleration (g)	Location	El centro (II)				Tianjin (IV)			
		Without WRCD	With WRCD-1C	With WRCD-2C	With WRCD-3C	Without WRCD	With WRCD-1C	With WRCD-2C	With WRCD-3C
0.8	P1	129.40	291.76	369.27	358.90	148.93	382.09	527.36	746.48
	P2	2554.40	1566.80	943.02	970.49	3690.30	1980.65	1557.05	1785.33
	P3	223.40	299.08	310.68	317.39	313.73	543.84	777.01	947.30

movable and fixed piers. The collective mechanical performance of the portable dock and the fixed pier can be achieved when a reasonable number of windings is selected.

3.5. Analysis of Different Seismic Input Responses. Tables 2, 3, and 4 enumerate the maximum acceleration response, maximum displacement response, and maximum strain response, respectively, of the pier top under the action of El Centro (class ii) and Tianjin (Class iv) waves under a ground motion input intensity of 0.8 g. The overall response of the structure is similar under these two types of ground motion input. For seismic waves with other input spectrum characteristics, the WRCD can coordinate the forces between the active and fixed piers and improve the overall mechanical performance of the structure.

4. Conclusions

The WRCD is proposed based on the principle of synergistic force between a continuous-beam bridge's main beam and the movable bearing pier. The synergistic power and shock-

absorption effects of a continuous-beam bridge with different pier heights are tested under earthquake conditions. In general, the test results showed that the WRCD has a good cooperative and isolation effectiveness for the model bridge and achieved the development purpose. However, the test results also showed that the pier height, the design parameters of the WRCD, and the input characteristics of ground motion will have different effects on the response of the structure. It is necessary to further study the design parameters of the WRCD in combination with the structural characteristics and the results of site seismic risk assessment, so as to achieve the optimal use effect of the WRCD. The findings of this research are as follows:

(1) WRCD can effectively improve the overall longitudinal stiffness of the model structure by increasing the input seismic energy of the system. The first-order natural vibration frequency of the network rises from 3.649 Hz without the device to 4.305 Hz with a single-winding device, and the overall synergistic force effect is significant. With increasing earthquake input intensity, the rotation axis of the WRCD rotates. After this rotation, the contribution of devices with different numbers of winding to the overall stiffness of the structure decreases, and the change in the natural vibration frequency of the structure with earthquake input intensity is not apparent.

(2) When the WRCD is applied, the acceleration response of the active pier is lower than that without the WRCD. The result is related to the pier height, as the influence of windings on high and low docks is slightly different. The acceleration response of the pier top with fixed pier increases compared with that without a static port, and the effect of the number of windings on the acceleration response of the pier top is inconsistent.

(3) When the WRCD is activated, the maximum displacement response of the pier top of the active pier increases and increases with the rise of the winding number. The displacement response of the main beam at the fixed pier is less than that without the device. The maximum reduction ratio is approximately 55%, and the displacement reduction effect of two windings is better than one or three windings.

(4) When the WRCD is applied, the maximum strain response of the active pier increases, and the strain response of the pier bottom is related to the pier height and increased with increasing windings. The strain response of the pier bottom with a fixed pier is about 40% without the device. The strain-response decrease increases with seismic input intensity for an endless number of windings. The stress of the movable and fixed piers can be coordinated by setting a reasonable number of windings.

(5) The overall response of the structure is similar under both seismic inputs studied, but the improvement result has a particular relationship with the ground motion input characteristics. For seismic waves with other input spectra, the WRCD can coordinate the forces between the active and fixed piers and improve the overall mechanical performance of the structure.

Data Availability

The data used to support the findings of this study are included within the article.

Conflicts of Interest

The authors declare that they have no conflicts of interest.

Acknowledgments

The authors thanked the workers, foremen, and safety coordinators of the main contractors for their participation. This work was supported by the National Natural Science Foundation of China (Grant no. 51778022).

References

[1] Y. T. Pang, "Seismic fragility assessment of an isolated multipylon cable-stayed bridge using shaking table tests," *Advances in Civil Engineering*, vol. 2017, Article ID 9514086, 12 pages, 2017.

[2] L. Yan, G. Li, and K. An, "Shaking table test of high pier and small radius curved bridge under multi-point excitation," *Advances in Civil Engineering*, vol. 2021, Article ID 6640755, 9 pages, 2021.

[3] Y. Liang, H. G. Wu, and T. W. Lai, "Dynamic response of bridge-landslide parallel system under earthquake," *Advances in Civil Engineering*, vol. 2022, Article ID 7508023, 16 pages, 2022.

[4] C. F. Wang, X. C. Chen, and X. S. Xia, "Parameters anslysis of the vibration distributing effect of longitudinal displacement limited continuous beam bridges," *Earthquake Engineering and Engineering Vibration*, vol. 32, no. 5, pp. 119–126, 2012.

[5] N. P. Kataria and R. S. Jangid, "Seismic protection of the horizontally curved bridge with semi-active variable stiffness damper and isolation system," *Advances in Structural Engineering*, vol. 19, no. 7, pp. 1103–1117, 2016.

[6] L. Y. Lu and C. C. Hsu, "Experimental study of variable-frequency rocking bearings for near-fault seismic isolation," *Engineering Structures*, vol. 46, pp. 116–129, 2013.

[7] A. Kashiwazaki, M. Tanaka, N. Tokuda, and T. Enomoto, "The earthquake and microtremor isolation floor system utilizing air springs and laminated rubber bearings," *TRANSACTIONS OF THE JAPAN SOCIETY OF MECHANICAL ENGINEERS Series C*, vol. 55, no. 512, pp. 847–852, 1989.

[8] L. P. Ren, S. H. He, and H. Y. Yuan, "Seismic fragility analysis of bridge system based on fuzzy failure criteria," *Advances in Civil Engineering*, vol. 2019, Article ID 3592972, 16 pages, 2019.

[9] H. X. Jia, J. Q. Lin, and J. L. Liu, "Bridge seismic damage assessment model applying artificial neural networks and the random forest algorithm," *Advances in Civil Engineering*, vol. 2020, Article ID 6548682, 13 pages, 2020.

[10] F. W. Wu, J. F. Luo, and W. Zheng, "Performance-based seismic fragility and residual seismic resistance study of a

long-span suspension bridge," *Advances in Civil Engineering*, vol. 2020, Article ID 8822955, 16 pages, 2020.

[11] Z. Q. Wang and J. P. Ge, "Application of viscous damper and lock-up devices in the seismic design of continuous girder bridges," *Journal of Shijiazhuang Railway Institute*, vol. 19, no. 1, pp. 5–9, 2010.

[12] Y. L. Zhang, X. C. Chen, and Z. H. Yan, "Research on seismic reduction performance of lock-up device applied to continuous girder bridges," *World Earthquake Engineering*, vol. 26, no. 2, pp. 48–52, 2010.

[13] L. Tang, Z. H. Cheng, X. Z. Ling, S. Cong, and J. Nan, "Preparation and performance of graphene oxide/self-healing microcapsule composite mortar," *Smart Materials and Structures*, vol. 31, no. 2, Article ID 025022, 2022.

[14] Z. H. Cheng and Y. S. Deng, "Bearing characteristics of moso bamboo micropile-composite soil nailing system in soft soil areas," *Advances in Materials Science and Engineering*, vol. 2020, Article ID 3204285, 17 pages, 2020.

[15] Y. S. Deng, Z. H. Cheng, and M. Z. Cai, "An experimental study on the ecological support model of dentate row piles," *Advances in Materials Science and Engineering*, vol. 2020, Article ID 6428032, 12 pages, 2020.

[16] X. S. Liu, W. Guo, and J. Z. Li, "Seismic study of skew bridge supported on laminated-rubber bearings," *Advances in Civil Engineering*, vol. 2020, Article ID 8899693, 17 pages, 2020.

[17] H. X. Gao, Y. Song, and W. T. Yuan, "Seismic design method of self-centring-segment bridge piers with tensile-type viscoelastic dampers," *Advances in Civil Engineering*, vol. 2021, Article ID 6688006, 12 pages, 2021.

[18] H. Su, Y. J. Hang, and Y. S. Song, "Seismic response of anchor + hinged block ecological slope by shaking table tests," *Advances in Materials Science and Engineering*, vol. 2018, Article ID 7684831, 13 pages, 2018.

[19] C. W. Yang, J. J. Zhang, and H. L. Qu, "Seismic earth pressures of retaining wall from large shaking table tests," *Advances in Materials Science and Engineering*, vol. 2015, Article ID 836503, 8 pages, 2015.